2018

OPTIMIZATION AND CONTROL OF AN ARRAY OF WAVE ENERGY CONVERTERS

Jianyang Lyu
Michigan Technological University, jlyu@mtu.edu

OPTIMIZATION AND CONTROL OF AN ARRAY OF WAVE ENERGY CONVERTERS

By

Jianyang Lyu

A REPORT

Submitted in partial fulfillment of the requirements for the degree of

MASTER OF SCIENCE

In Mechanical Engineering

MICHIGAN TECHNOLOGICAL UNIVERSITY

2018

This report has been approved in partial fulfillment of the requirements for the Degree of MASTER OF SCIENCE in Mechanical Engineering.

Department of Mechanical Engineering-Engineering Mechanics

Thesis Co-advisor:	*Dr. Ossama Abdelkhalik*
Thesis Co-advisor:	*Dr. Lucia Gauchia*
Committee Member:	*Dr. Andrew Barnard*
Committee Member:	*Dr. Ali Ebnenasir*
Department Chair:	*Dr. William Predebon*

Contents

List of Figures

List of Tables

List of Abbreviations

BEM	Boundary Element Method
GA	Genetic Algorithm
nWEC	Number of Wave Energy Converters
OWC	Oscillating Water Column
WEC	Wave Energy Converter

Abstract

This study explored optimal configuration of both the array layout and the dimension of each WEC in the array. The array contains heaving buoys with full interaction and exact hydrodynamics. Optimization of dimension was done on each WEC in the array with a given optimal layout, and a higher q-factor was achieved. Both impedance matching optimal control and derivative control were employed, which provides both theoretical maximum energy and a more realistic case. Then the work was expanded to optimization of both the array layout and the dimension of each WEC in the array. An average of 39.21% higher q-factor can be achieved with the optimal control and an average of 8.87% higher q-factor can be achieved with the derivative control. Optimization of both the layout of array and the dimension of each WEC was done under irregular wave. The irregular wave was formulated with Bretschneider spectrum. Preliminary results from the irregular wave optimization indicates an asymmetric layout of array is needed.

Chapter 1

Introduction

1.1 Background and motivation

It is well recognized that traditional fossil fuel energy is limited in the global storage after the early exploration by Hubbert and King [27]. On the other hand, due to the foreseeable limit of fossil fuels and the more strict requirement on emissions, automotive industry is moving forward the production of full-electric and hybrid electric vehicles, which leads to a higher demand of electrical energy. This calls for development of effective replacement for energy production that is free of the dependence of fossil fuel. Currently, supplementary sources for electric power production includes nuclear power, hydro-power, bio-power, geothermal power, solar power and wind power. The

total renewable electrical power capacity is 2017 GW in 2016, and the capacity of hydro power is 1096 GW which is more than half of the total capacity[29](nuclear power excluded.) Among all hydro power production by the end of 2016, the global ocean energy capacity was 536 MW.

Aside from the growing market and industry of ocean wave energy, the total theoretical potential from just wave energy is estimated to be 29.5 PWh/yr in 2010, which covers more than the entire U.S. electricity power consumption in 2008[57].

The need for renewable energy, the increasing capacity of energy market, the large potential in ocean waves, all calls for the development of more efficient design and control of ocean wave energy devices and farms.

Current study on WEC array mostly assumed identical WEC with the same mode of motion. The previous studies[16],[46] and [1] indicates that both heave mode and pitch mode can have similar energy potential in wave energy harvesting. Also as discussed in literature[25], the dimension has an impact on array performance that can not be ignored. On the control of WEC array, although several control algorithms have been evaluated[21][46][6], the optimization of both control, layout of the array and the dimension of each buoy remains unexplored [6]. The main problems in the research of WEC array are:

† The optimization of WEC array mostly focuses on layout of array.

† Buoys used in WEC array study are assumed to be identical and contain only one mode of motion

† Optimal control of WEC array has not been done on arrays that contain WEC of different dimension and modes.

1.2 Research objectives

The objectives of this research will be:

† Optimize both dimension and layout for an array of wave energy converters

Chapter 2

Literature Review

2.1 Factors in the design of array of wave energy converters

Global layout of the WEC array, the size of array, and the shape and dimension of each device, along with the wave profile including wave direction and sea states, all have great impact on the array performance[17][25][23]. The effect of incoming wave direction was studied in [17][12][55][14]. The integration of q-factor calculated from all directions around the array is a constant number of one. The interaction of buoys in the array of an arbitrary layout was studied in [11][18][22]. The park effect has been studied by Babarit[1], and the separation distance was found to be $500m$ such

that people can neglect park effect.

Besides the separation distance, size and shape of WEC are also significant factors in designing arrays. Earlier study of the compact array has found that the center buoy always has a higher response compared to the other buoys in the array [22]. The impact from varying separation distance of each device in the array is studied by Korde and Ringwood[46] with arrays containing 2,3 and 4 buoys with four arbitrary geometries of the layout. A 40% higher q-factor was found when control and separation distance were selected properly. Recently, an expanded multiple scattering method is developed by Goteman[24] which assumes cylindrical device while allowing the size of each device to change. This study showed an improved array performance with buoys of different dimensions and great potential in designing large WEC arrays.

2.2 Optimization of WEC array

Since the early research of Budal[9], Evans[53] and Falnes[15], optimal layout of an array has been studied under many cases and remains a popular topic in array design. Layout optimization has been done under both regular and irregular wave to find optimal layout for an array of given size. Due to the complex nature of hydrodynamic interaction[36], global optimization is required to find the optimal layout that provides constructive interaction. Similar to Fitzgerald's study[17], Child[12]

modified the layout optimization problem and formulates a local optimization. The parabolic intersection method Child developed is more efficient but less accurate than traditional GA. Moarefdoost[36] borrowed the idea and further increased calculation speed by using point absorber approximation from Budal[9] rather than using exact hydrodynamics. Meanwhile, layout optimization is conducted by McGuinness with the constrains of device motion[33].

2.3 Modeling the hydrodynamics of WEC array

In array optimization problems, modeling exact hydrodynamic interaction is well recognized to consume the most computational power. In the review of park effect in WEC arrays, Babarit[2] concludes that BEM solvers provide the most accurate hydrodynamics with the least speed. On the other hand, analytical approximation, such as point absorber approximation, limits the ability to study more complex configuration of arrays. Thus, most of the array layout studies focus on arrays of identical buoys which holds a high level accuracy even with analytical approximation. Machine learning methods have also been borrowed to search for an optimal layout of flap-type WEC array[47].

2.4 Control of WEC array

The early optimal control of the WEC array was studied in [20]. A realistic limit of power production from an array was developed using complex conjugate approximation.The q-factor was studied for both terminator and attenuator array configurations. When designing the optimal controller for a given WEC array, the device can either share information and communicate with each other with global control, or access only information and prediction from sensors mounted on itself with independent control [46][3][21]. In [46] and [21], four different arbitrary layouts were studied. Optimal control was evaluated at different separation distance for each layout. With the assumption of large separation distance, Nielsen proposed a frequency domain optimal control that is independent of array layout[41].

Chapter 3

Wave Energy Converter Dynamics

3.1 Dynamics of an isolated wave energy converter

With the assumption of in-viscid, in-compressible and irrotational fluid, the linear potential flow theory can be applied to model the fluid around an object[16][40], which is the wave energy converter in this study. The total velocity potential around a wave energy converter contains three components: incident wave potential, diffracted wave potential and radiated wave potential. With linearity of each potential component, the total force from ocean wave acting on each WEC device is expressed as a summation of wave excitation force, hydro-static force and radiation force. Where incident wave potential and diffracted wave potential together contribute to what we

call wave excitation force, and radiated wave potential results in radiation force. For an isolated WEC oscillating in heaving motion in ocean, the equation of motion is written in Eq.3.1.

$$m\ddot{x} = f_e + f_r + f_s + f_c \tag{3.1}$$

Where f_e, f_r, f_s, f_c denotes excitation force, radiation force, hydro-static force and control force respectively. $\ddot{x}$ is the heave acceleration of the buoy. As described above, the wave excitation force has two components. The force generated only from incident wave potential and ignoring the diffracted wave due to the existence of the buoy is called Froude-Krylov force[16][46]. The force generated only from the potential of diffracted waves due to the existence of the buoy is called diffraction force. Each force can be computed from integrating the resulting pressure around the WEC wetted surface[46].

$$f_e = i\omega\rho \iint_S (\hat{\phi_0} + \hat{\phi_D})\vec{n}dS \tag{3.2}$$

Where i is the symbol of the complex number, ω is the frequency of the incoming ocean wave, and ρ is water density. ϕ_0 and ϕ_D are incident wave potential and diffracted wave potential respectively. $\vec{n}$ is normal vector to the wetted surface of the buoy and S is the wetted surface area of the buoy. Since there's no analytical solution to this integration problem, either the analytical approximation or the numerical boundary element solvers need to be employed to solve for the excitation force. In this study the numerical BEM solver Nemoh will be employed to solve for the exact hydrodynamics of the WEC array. The resulting expression for the excitation force is shown in Eq.3.3

$$f_{ex}(\omega) = \Re((a(\omega) + ib(\omega))\eta(\omega)e^{\phi(\omega)}) \tag{3.3}$$

Where a and b are the frequency hydrodynamic coefficients computed from Nemoh. η is the amplitude of the surface elevation of incoming wave and ϕ is the phase of it.

Hydro-static force is the difference of the buoyancy force and the gravitational force. It is linear to the intersection surface area of the wave energy converter and it is assumed to be a static force in this study. A is the intersection area of the buoy.

$$f_s = \rho g A x \tag{3.4}$$

The expression describing the radiation force in heave motion is given by the Cummins' equation[58].

$$f_r = m_a(\infty)\ddot{x} + \int_0^\infty h_\tau(\tau)\dot{x}(t-\tau)d\tau \tag{3.5}$$

In Eq.3.5, f_r and x are the radiation force and the displacement of the buoy, where $\dot{x}$ and $\ddot{x}$ are buoy velocity and acceleration respectively. With the Fourier transformation, the convolution can be solved in the frequency domain and we can express the total radiation force with the frequency dependant coefficients:

$$f_r = m_a(\omega)\ddot{x} + b_r(\omega)\dot{x} \tag{3.6}$$

Similar to the solution of excitation force, BEM solver Nemoh will be employed to solve for the hydrodynamic coefficients $m_a(\omega)$ and $b_r(\omega)$. Once the frequency dependant coefficients are obtained, one can calculate radiation force in the time domain by doing the inverse Fourier transformation on it.

3.2 WEC array dynamics

The equation of motion for WEC array in the compact matrix form[1] is shown in Eq.3.7.

$$(\mathbf{M} + \mathbf{M_a}(\omega))\ddot{\vec{\mathbb{X}}} + (\mathbf{B_v} + \mathbf{B_r}(\omega))\dot{\vec{\mathbb{X}}} + \mathbf{K_h}\vec{\mathbb{X}} = \vec{\mathbb{F}_{ex}} + \vec{\mathbb{F}_c} \tag{3.7}$$

$\mathbf{M}$ and $\mathbf{M_a}(\omega)$ are the mass and added mass matrices of the array, $\mathbf{B_v}$ and $\mathbf{B_r}(\omega)$ are the viscous and radiation damping matrices, and $\mathbf{K_h}$ is the hydro-static coefficient matrix of the array. $\mathbf{M}$, $\mathbf{B_v}$ and $\mathbf{K_h}$ are the static force coefficient matrices and contain only diagonal elements. In the radiation coefficient matrices $\mathbf{M_a}(\omega)$ and $\mathbf{B_r}(\omega)$, the hydrodynamic interaction is shown by off-diagonal elements.

$$M_{a_{array}}(\omega) = \begin{bmatrix} m_{a_{11}}(\omega) & m_{a_{12}}(\omega) & \dots & \dots & m_{a_{1n}}(\omega) \\ m_{a_{21}}(\omega) & m_{a_{22}}(\omega) & m_{a_{23}}(\omega) & \dots & m_{a_{2n}}(\omega) \\ \vdots & \vdots & \vdots & \ddots & \vdots \\ m_{a_{n1}}(\omega) & \dots & \dots & \dots & m_{a_{nn}}(\omega) \end{bmatrix}$$

$$B_{r_{array}}(\omega) = \begin{bmatrix} b_{r_{11}}(\omega) & b_{r_{12}}(\omega) & \dots & \dots & b_{r_{1n}}(\omega) \\ b_{r_{21}}(\omega) & b_{r_{22}}(\omega) & b_{r_{23}}(\omega) & \dots & b_{r_{2n}}(\omega) \\ \vdots & \vdots & \vdots & \ddots & \vdots \\ b_{r_{n1}}(\omega) & \dots & \dots & \dots & b_{r_{nn}}(\omega) \end{bmatrix} \tag{3.8}$$

Vector $\mathbb{X}$ is the displacement vector of the array. $\mathbb{F}_{ex}$ and $\mathbb{F}_c$ are the excitation force and control force vector respectively. All hydrodynamic coefficients can be calculated using the numerical BEM solver Nemoh.

3.3 Control of an array of wave energy converters

To extract energy from the WEC array, a control algorithm that can provide the proper control force is necessary. To obtain the preliminary results from simulation, two different control strategies are employed. One unconstrained impedance matching control reveals the theoretical optimum power absorption, and one passive derivative

control produces a control force proportional to the velocity.

Considering an isolated oscillating system with only the heave motion, the optimal control force without constraints is given by matching impedance of the system [16]:

$$\overrightarrow{\mathbb{F}_c} = \frac{1}{2}\mathbf{B_r}(\omega)^{-1}\overrightarrow{\mathbb{F}_{ex}} \tag{3.9}$$

The optimum power for the array is then found to be [16]:

$$P_{max} = \frac{1}{8}\overrightarrow{\mathbb{F}_{ex}}^{*}\mathbf{B_r}(\omega)^{-1}\overrightarrow{\mathbb{F}_{ex}} \tag{3.10}$$

Note that in Eq.3.10, $\overrightarrow{\mathbb{F}_{ex}}$ is the hydrodynamic excitation force coefficient calculated from the BEM solver assuming an unity wave input. Physically both $\mathbf{M_a}(\omega)$ and $\mathbf{B_r}(\omega)$ are symmetric since the radiation impedance between any two bodies are the same with the unit velocity. It implies that $m_{a_{ij}}(\omega) = m_{a_{ji}}(\omega)$ and $b_{r_{ij}}(\omega) = b_{r_{ji}}(\omega)$ where i and j are the index for WECs in the array. A power calculated from Eq.3.10 is always real. But with the BEM solver such as Nemoh, there is a numerical error between $m_{a_{ij}}(\omega)$ and $m_{a_{ji}}(\omega)$ when WECs in the array are no longer identical. In the

later simulation, only half of the hydrodynamic matrix is carried into calculation as a correction to this problem. With the optimal control, this power can be considered as theoretical maximum absorbed power from the array.

The second control implemented for preliminary research is the passive/derivative control, with the control force proportional to the array velocity (Eq.3.11).

$$\overrightarrow{\mathbb{F}_c} = \mathbf{K_d}\,\overrightarrow{\dot{\mathbb{X}}} \tag{3.11}$$

The coefficient matrix $\mathbf{K_d}$ have only the diagonal elements of $\mathbf{B_r}(\omega)$, and the power from array is written as Eq.3.12. The control force needs only the information from the buoy itself but not from the entire array.

$$\begin{aligned} P_{passive} &= -\sum_{i=1}^{i=N} f_{c_i}\dot{x}_i \\ &= -\sum_{i=1}^{i=N} k_{d_i}\dot{x}_i\dot{x}_i \\ &= \omega^2 \sum_{i=1}^{i=N} k_{d_i}|\bar{x}_i|^2 \end{aligned} \tag{3.12}$$

Chapter 4

Optimization of an array of wave energy converters

The wave energy converter arrays we considered in this research contain only cylindrical heaving WEC. As discussed in the literature review, WEC array problems have more than a few local optimums in the search domain[36]. Local optimization algorithms such as the quadratic programming will fail in finding the optimal solution. Thus, it is necessary to employ the global optimization algorithms to solve for the optimal solution. In this chapter, Genetic Algorithm is employed to solve for the optimal solution to the WEC array optimization problem. The formulation of the

objective function is shown in Eq.4.1

$$\max_{dimension} q = \frac{Total\,power\,from\,array}{Total\,power\,summed\,from\,each\,isolated\,WEC} \tag{4.1}$$

4.1 Optimization of the dimension of each buoy in the WEC array with Genetic Algorithm

In this section, the q-factor of the array is optimized with the design parameters selected as the radius of each buoy in the array. The layout of the array is optimized separately with the equation of q-factor simplified with the point absorber approximation[36]. The expression of q-factor with the point absorber approximation is given in [9].

$$q = \frac{1}{N}\mathbf{L}^{*}\mathbf{J}^{-1}\mathbf{L} \tag{4.2}$$

The column vector **L** contains the polar coordinates for each WEC in the array. and **J** is the first kind Bessel function of order zero to approximate power with relative distance of buoys in the array.

$$L_m = e^{ikd_m \cos\beta - \alpha_m}$$
$$J_{mn} = J_0(kd_{mn}) \tag{4.3}$$

In Eq.4.3, m and n are the indices of buoys in the array. (α_m, d_m) is the polar coordinate of each WEC in the array. k is the wave number associated with the wave frequency and β is the angle of the wave direction.

With the wave direction of 0°, the optimized layouts for arrays that contain three, five and seven WECs are solved in the literature[36] and the result is shown in Fig.4.1

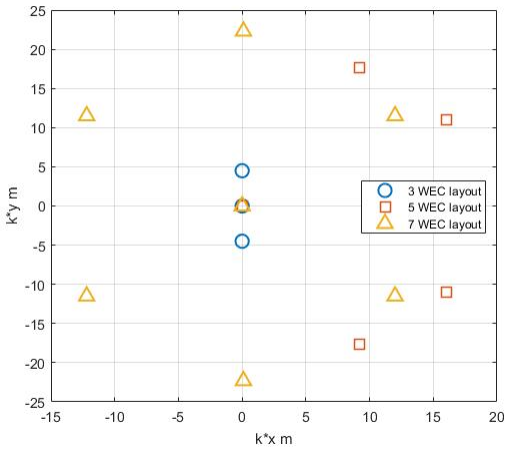

Figure 4.1: Optimal layout for array of 3 WEC, 5 WEC and 7 WEC[36]

Once the optimal layout is obtained, it will be used for optimization of the dimension of each buoy in the array. The variables that define the dimension of the cylindrical buoys are:

1. radius of each buoy $R_1, R_2, ...R_n$

2. draft of each buoy $D_1, D_2, ...D_n$

Here we constrained the design variables by fixing the mass of each device. This leads to a constant submerged volume of each buoy. The constraint can be written as:

$$V_i = \pi R_i^2 D_i = constant \tag{4.4}$$

With the constraint above, the design variables are defined as the radius of each buoy $R_1, R_2, ...R_n$ with the draft height of each buoy defined as $D_i = \frac{V_i}{\pi R_i^2}$.

The initial volume of each buoy is selected as $1\,m^3$. The formulation of the optimization is written as:

$$\begin{aligned} &\underset{dimension,layout}{max} \quad q = \frac{P_{array}}{\sum P_i} \\ &s.t. \qquad D_i = \frac{1}{\pi R_i^2} \quad \forall \quad i = 1, 2, 3, ... \\ &R_i \subset [0.5, 2]m \quad \forall \quad i = 1, 2, 3, ... \end{aligned} \tag{4.5}$$

Genetic Algorithm built in MATLAB® is employed to solve this problem with the settings shown in Table4.1.

Items	Value
Max generation	100
Max population	10*nWEC
Increment in searching R_i	0.15m

Table 4.1
Settings of Genetic Algorithm built in MATLAB®

4.2 Optimization of both dimension and layout of WEC array

The mathematical formulation of optimization of both dimension and layout of a WEC array is presented in this section. Similar to the optimization in section 4.1, the objective is to maximize the q-factor of an WEC array. The design parameters are selected as both the layout of the array and the dimension of each WEC device. Since the optimal layout of a WEC array is symmetric under the point absorber approximation[17], another constraint on the location of each WEC needs to be considered. In this study, only optimal control is applied to calculate the power from the array. This optimization is done only on the array of three WECs.

The design variables are the radius of each buoy R_1, R_2, R_3, and the location of each buoy $[x_1, y_1], [x_2, y_2], [x_3, y_3]$ in Cartesian coordinate. Applying the constraint of

symmetric layout, the location of the first buoy is fixed at the origin, the location of the second buoy is on the upper half plain and the location of the third buoy is on the lower half plain. The formulation of this optimization is written as:

$$
\begin{aligned}
&\underset{dimension,layout}{max} \quad q = \frac{P_{array}}{\sum P_i} \\
&s.t. \qquad D_i = \frac{1}{\pi R_i^2} \quad \forall \quad i = 1,2,3 \\
&R_i \subset [0.5, 2]m \quad \forall \quad i = 1,2,3 \\
&x_1 = y_1 = 0m \\
&x_2, x_3 \subset [-10, 10]m \\
&y_2 \subset [4.5/k - 50, 4.5k + 50]m \quad \& \quad y_3 \subset [-4.5/k - 50, -4.5k + 50]m
\end{aligned}
\tag{4.6}
$$

Where k is the wave number and $[0, \pm 4.5k]m$ is the optimal location for the second and the third buoy solved with point absorber approximation from section 4.1.

Chapter 5

Optimization Results of both dimension and layout of an array of wave energy converters

The initial WEC array layout is shown in Fig.4.1. The initial dimension for all WECs are selected as $R = 1m$, $D = 1m$. The wave number used for comparison is $k = 0.2$. The wave direction is set to $\beta = 0°$ for all simulation. Hydrodynamics BEM solver Nemoh is employed to compute the exact hydrodynamics for all simulation.

Since the product of kR remains unchanged, the q-factor calculated using the initial setup of the array is verified to be the same as the one from the literature[36].

Also, since the point absorber approximation is used in the literature[36], we need to validate the results using the exact hydrodynamic coefficients from Nemoh. The comparison is shown in Table5.1. Since $kR = 0.2$ remains the same, the resulting q-factor did not change. From the Table5.1 we can see that all calculated q-factors are close to each other, and the difference between approximation and Nemoh solution is small.

tests	q	k	R	D	kR	nWEC	hydrodynamics
Ref[36]	1.9848	0.04	5m	20m	0.2	3	approx.
test 1	1.9846	0.2	1m	1m	0.2	3	Nemoh
test 2	1.9822	0.04	5m	20m	0.2	3	Nemoh

Table 5.1
Compare the literature result with the Nemoh results

5.1 Optimization of only the dimension of each buoy in the WEC array

With the layout shown in Fig.4.1, and the mathematical formulation in Chapter 4 section4.1, optimization of the dimension of each WEC in the arrays of three, five and seven buoys are done with both the optimal control and the passive control. Optimization results using the optimal control are shown in Fig.5.1, and results using the derivative are shown in Fig.5.2. For the array of three WECs, buoy 1,2,3 refer to the buoy on the center, the buoy on the top and the buoy on the bottom. For the array of five WECs, buoy 1 to 5 are the buoy on the center, the upper buoy on the

2nd column, the lower buoy on the 2nd column, the upper buoy on the 3rd column, and the lower buoy on the 3rd column respectively. For the array of seven WECs, buoy 1 is on the center, buoy 2,4,6 are the upper buoys on column 1,2,3, and buoy 3,5,7 are the lower buoys on each column.

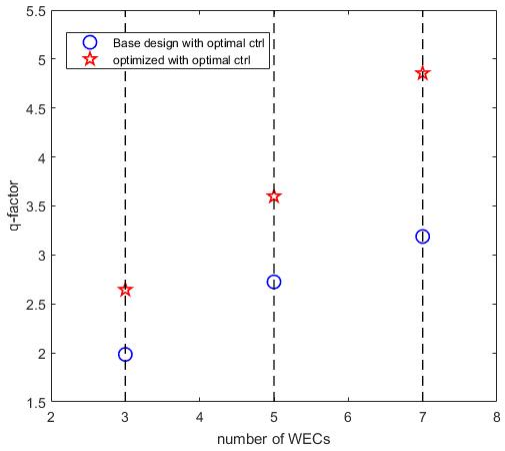

Figure 5.1: The q-factor optimized using optimal control. The circles represent the results with initial set up, and pentagrams represent the results with optimized dimensions

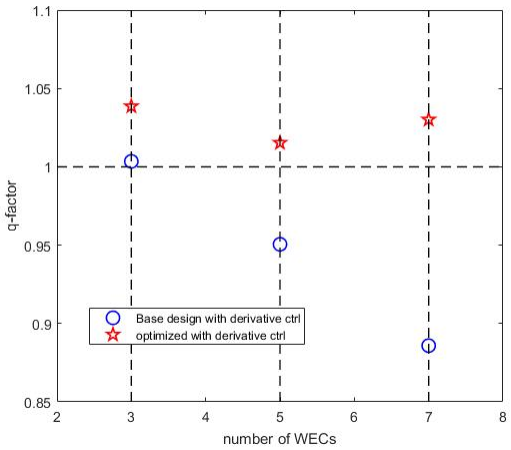

Figure 5.2: The q-factor optimized using passive control. The circles represent the results with initial set up, and pentagrams represent the results with optimized dimensions

As the results in Fig.5.1 and Fig.5.2 indicate, in both cases, a higher q-factor is achieved by optimizing the dimension of each device. The optimized q-factor is 39.21% higher using the optimal control and it is 8.87% higher using the derivative control.

With the initial setup, arrays using the derivative control do not perform as well as arrays using the optimal control. This is because the selected layout is optimized with the point absorber approximation which assumes the optimal control. But with optimization of the dimension, the q-factors for all three arrays are above one. It indicates a constructive coupling effect between each buoy in the array (Fig.5.2.)

On Fig.5.3, the red circles are optimized radius of each buoy and the black circles are the initial radius of each buoy. For the tests with the optimal control, we can see that the center buoys in all three arrays have the largest possible radius, and almost all other buoys have smallest possible radius. For the tests with the derivative control, the center buoys have the largest radius, and the buoys on the third column have the 2nd largest radius.

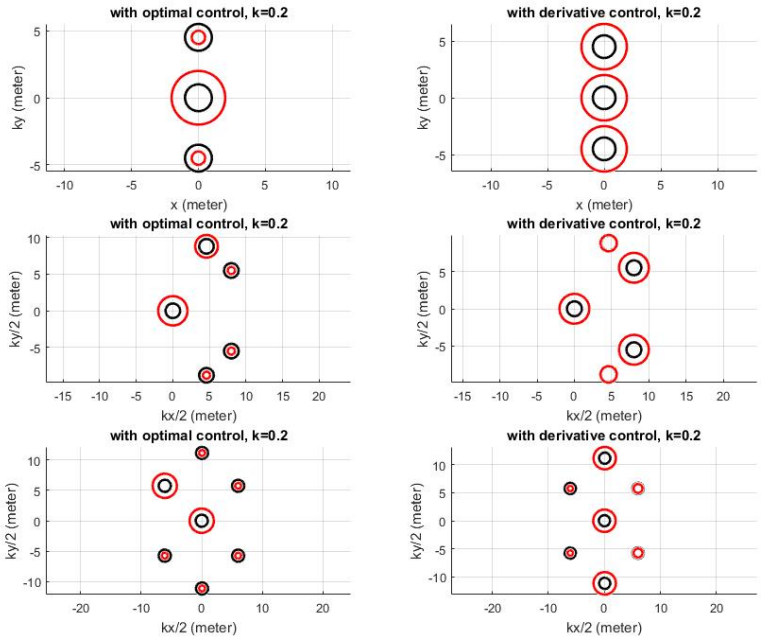

Figure 5.3: Optimized dimensions for each WEC in the array. Figures on the left are optimized dimensions using the optimal control. Figures on the right are results using derivative control

5.2 Optimization of both dimension of each WEC and layout of the array

The mathematical formulation of this optimization is shown in Chapter 4 section 4.2. The optimization result is shown in Table.5.2. The solution from optimization with GA is the same as the optimal layout from literature. At different wave number, the optimal location for the second and the third buoy are always $[0, \pm 4.5k]m$ respectively. For the sake of reducing computation time, the search step of GA is set to be 1 meter. The q-factor from this optimization is then smaller than the q-factors in Table.5.1.

When calculating q-factor with exact coordinates of $[0, \pm 4.5k]m$ as the layout, the q-factor is the same as results in Table.5.1.

test	q	k	WEC2 (m)	WEC3 (m)	x constraint(m)
Ref[36]	1.98	0.04	[0,4.5/k]	[0,-4.5/k]	[-10,10]
case1	2.10	0.2	[0,22]	[0,-22]	[-10,10]
case2	2.08	0.3	[0,15]	[0,-15]	[-10,10]
case3	2.07	0.04	[0,109]	[0,-109]	[-10,10]
case4	2.07	0.04	[0,109]	[0,-109]	[-100,100]

Table 5.2
Compare optimization results with different wave numbers. The location constraint shown is in x direction

This result above showed that this optimization formulation can solve for the optimal solution when the design variables are the array layout and the dimension of buoys.

5.3 Optimization of both dimension of each WEC and layout of the array under irregular wave

When the input wave is irregular and thus contains more than one frequency, the optimization with GA is computational expansive when using the exact hydrodynamics. Due to this limitation, only 7 population is used for the optimization under irregular wave. The irregular wave is constructed with the bretschneider spectrum. The significant wave height is $1.158m$ and the peak period is $8\,sec$. Optimization result using optimal control is shown on Fig.5.4. The q-factor calculated from this setup is 1.77.

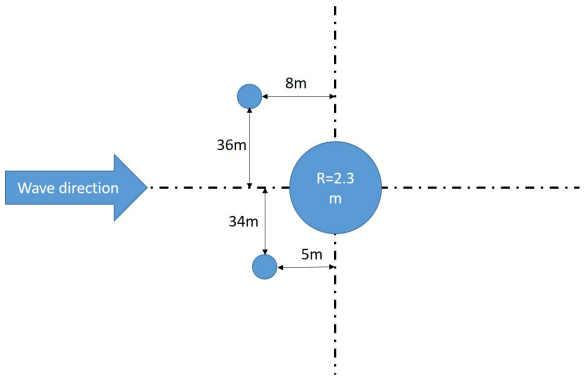

Figure 5.4: Optimized layout and dimension for array of 3 WECs under irregular wave using optimal control

This layout is not symmetric but we can see that the center buoy was optimized to be critical important over the buoys on the side. This is the same behavior that has been observed for the tests with regular wave.

Optimization result using passive control is shown in Fig.5.5.

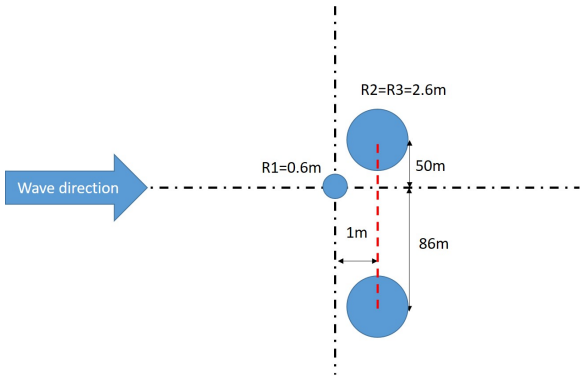

Figure 5.5: Optimized layout and dimension for array of 3 WECs under irregular wave using passive control

	regular wave	irregular wave	initial
Optimal control	2.67	1.77	1.98
Passive control	1.04	1.07	1.00

Table 5.3
Compare the optimized q-factors from both regular and irregular wave

When optimizing the array layout and the dimension of buoys under irregular wave using the optimal control, the resulting dimension and layout has similar characteristics with the optimization solution from regular wave. Computation time for the irregular wave optimization increased significantly compared with the regular wave optimization.

Chapter 6

Future Research on Optimization of WEC array

As discussed in Chapter1 section1.2, the study will be expanded to include both regular and irregular wave optimization and simulation. Then the modes of motion of each WEC in the array can be considered in the optimization. Collective control can be implemented on the optimized array.

6.1 Optimization of both dimension and layout for an array of wave energy converters

Optimization will be done under both regular and irregular input waves. As the results shown in Chapter5, a higher q-factor is achieved by optimizing both dimension and layout of a WEC array under the regular wave. The irregular wave is more complex and increases the computational cost significantly during the calculation of the exact hydrodynamics of the array. Although results and analysis can be achieved using the BEM solver Nemoh, a more computational efficient tool for computing the hydrodynamics needs to be implemented to increase the efficiency of the optimization. A multiple scattering method[24] can be employed to solve for the hydrodynamics for an array of cylindrical buoys.

6.2 Optimization of mode for an array of wave energy converters

The analysis of the WEC array of flap-type or OWC devices has been done in the literature*citehere*. The study needs to be expanded, such that an array can contain

buoys of different modes of motion. Simulation needs to be done to study the interaction of WEC of different modes in the same array. Then we can optimize the mode of motion for each WEC in the array along with the optimization of dimension and layout of it.

6.3 Optimal control of an array of wave energy converters

In previous optimization of both dimension and layout of the array, we assumed two scenarios using two control algorithms. The results indicate a strong correlation between the control strategy, the layout and the dimension of buoys. Since the research of the control of WEC array in the literature[46][3] mostly assumes an arbitrary layout of the array and identical WEC, it is of critical importance to evaluate the performance of different controllers on an optimal layout with the optimal dimension for each WEC in the array. Also, the collective control needs to be implemented on the array of WECs of different modes of motion.

References

[1] A. Babarit. Impact of long separating distances on the energy production of two interacting wave energy converters. *Ocean Engineering*, 37(8):718 – 729, 2010.

[2] A. Babarit. On the park effect in arrays of oscillating wave energy converters. *Renewable Energy*, 58:68 – 78, 2013.

[3] G. Bacelli, P. Balitsky, and J. V. Ringwood. Coordinated control of arrays of wave energy devices x2014;benefits over independent control. *IEEE Transactions on Sustainable Energy*, 4(4):1091–1099, Oct 2013.

[4] A. Bahaj and L. Myers. Shaping array design of marine current energy converters through scaled experimental analysis. *Energy*, 59:83 – 94, 2013.

[5] H. Bailey, B. Robertson, and B. Buckham. Variability and stochastic simulation of power from wave energy converter arrays. *Renewable Energy*, 115:721 – 733, 2018.

[6] P. Balitsky. Modelling controlled arrays of wave energy converters. June 2013.

[7] B. Borgarino, A. Babarit, and P. Ferrant. Impact of wave interactions effects on energy absorption in large arrays of wave energy converters. *Ocean Engineering*, 41:79 – 88, 2012.

[8] B. Borgarino, A. Babarit, and P. Ferrant. Impact of wave interactions effects on energy absorption in large arrays of wave energy converters. *Ocean Engineering*, 41:79 – 88, 2012.

[9] Budal. Theory for absorption of wave power by a system of interacting bodies. *Journal of Ship Research*, 21(4):248 – 253, 1977.

[10] I. Chatjigeorgiou and V. Katsardi. Hydrodynamics and near trapping effects in arrays of multiple elliptical cylinders in waves. *Ocean Engineering*, 157:121 – 139, 2018.

[11] W. Chen, F. Gao, X. Meng, and J. Fu. Design of the wave energy converter array to achieve constructive effects. *Ocean Engineering*, 124:13 – 20, 2016.

[12] B. Child and V. Venugopal. Optimal configurations of wave energy device arrays. *Ocean Engineering*, 37(16):1402 – 1417, 2010.

[13] F. C. da Fonseca, R. Gomes, J. Henriques, L. Gato, and A. Falco. Model testing of an oscillating water column spar-buoy wave energy converter isolated and in array: Motions and mooring forces. *Energy*, 112:1207 – 1218, 2016.

[14] A. de Andrs, R. Guanche, L. Meneses, C. Vidal, and I. Losada. Factors that influence array layout on wave energy farms. *Ocean Engineering*, 82:32 – 41, 2014.

[15] J. Falnes. Radiation impedance matrix and optimum power absorption for interacting oscillators in surface waves. *Applied Ocean Research*, 2(2):75 – 80, 1980.

[16] J. Falnes. *Ocean Waves and Oscillating Systems*. Cambridge University Press, 2002.

[17] T. G. Fitzgerald, C. A preliminary study on the optimal formation of an array of wave power devices. *In:Proceedings of the 7th European Wave and Tidal Energy Conference*, 2007.

[18] F. F. Flavi, A. Babarit, and A. Clment. On the numerical modeling and optimization of a bottom-referenced heave-buoy array of wave energy converters. *International Journal of Marine Energy*, 19:1 – 15, 2017.

[19] F. F. Flavi, C. McNatt, F. Rongre, A. Babarit, and A. Clment. A numerical tool for the frequency domain simulation of large arrays of identical floating bodies in waves. *Ocean Engineering*, 148:299 – 311, 2018.

[20] M. Folley and T. Whittaker. The effect of sub-optimal control and the spectral wave climate on the performance of wave energy converter arrays. *Applied Ocean*

Research, 31(4):260 – 266, 2009. Renewable Energy: Leveraging Ocean and Waterways.

[21] P. B. Garcia-Rosa, G. Bacelli, and J. V. Ringwood. Control-informed optimal array layout for wave farms. *IEEE Transactions on Sustainable Energy*, 6(2):575–582, April 2015.

[22] X. Garnaud and C. C. Mei. Comparison of wave power extraction by a compact array of small buoys and by a large buoy. *IET Renewable Power Generation*, 4(6):519–530, November 2010.

[23] M. Giassi and M. Gteman. Layout design of wave energy parks by a genetic algorithm. *Ocean Engineering*, 154:252 – 261, 2018.

[24] M. Gteman. Wave energy parks with point-absorbers of different dimensions. *Journal of Fluids and Structures*, 74:142 – 157, 2017.

[25] M. Gteman, J. Engstrm, M. Eriksson, and J. Isberg. Optimizing wave energy parks with over 1000 interacting point-absorbers using an approximate analytical method. *International Journal of Marine Energy*, 10:113 – 126, 2015.

[26] M. Gteman, J. Engstrm, M. Eriksson, J. Isberg, and M. Leijon. Methods of reducing power fluctuations in wave energy parks. *Journal of Renewable and Sustainable Energy*, 6(4):043103, 2014.

[27] Hubbert and M. King. Nuclear energy and the fossil fuels. Shell Oil Company/American Petroleum Institute, Mar 1956.

[28] P. T. Jacobson, G. Hagerman, and G. Scott. Mapping and assessment of the united states ocean wave energy resource. 12 2011.

[29] e. a. Janet L. Sawin. Ren21 annual report 2017. Sep 2017.

[30] . Y. D. Kagemoto, H. Interactions among multiple three-dimensional bodies in water waves: An exact algebraic method. *Journal of Fluid Mechanics*, 166:189–209, 1986.

[31] D. Khojasteh, S. M. Mousavi, W. Glamore, and G. Iglesias. Wave energy status in asia. *Ocean Engineering*, 169:344 – 358, 2018.

[32] Z. Liu, N. Qu, Z. Han, J. Zhang, S. Zhang, M. Li, and H. Shi. Study on energy conversion and storage system for a prototype buoys-array wave energy converter. *Energy for Sustainable Development*, 34:100 – 110, 2016.

[33] J. P. McGuinness and G. Thomas. The constrained optimisation of small linear arrays of heaving point absorbers. part i: The influence of spacing. *International Journal of Marine Energy*, 20:33 – 44, 2017.

[34] J. C. McNatt, V. Venugopal, and D. Forehand. A novel method for deriving the diffraction transfer matrix and its application to multi-body interactions in water waves. *Ocean Engineering*, 94:173 – 185, 2015.

[35] F. J. Mendez, P. Camus, R. Medina, and A. Cofino. Analyzing the multidimensional wave climate with self organizing maps. In *OCEANS 2009-EUROPE*, pages 1–9, May 2009.

[36] M. M. Moarefdoost, L. V. Snyder, and B. Alnajjab. Layouts for ocean wave energy farms: Models, properties, and optimization. *Omega*, 66:185 – 194, 2017. New Research Frontiers in Sustainability.

[37] L. Myers and A. Bahaj. An experimental investigation simulating flow effects in first generation marine current energy converter arrays. *Renewable Energy*, 37(1):28 – 36, 2012.

[38] J.-R. Nader, A. Fleming, G. Macfarlane, I. Penesis, and R. Manasseh. Novel experimental modelling of the hydrodynamic interactions of arrays of wave energy converters. *International Journal of Marine Energy*, 20:109 – 124, 2017.

[39] J.-R. Nader, S.-P. Zhu, and P. Cooper. Hydrodynamic and energetic properties of a finite array of fixed oscillating water column wave energy converters. *Ocean Engineering*, 88:131 – 148, 2014.

[40] J. N. Newman. *Marine Hydrodynamics*. MIT Press, 1935.

[41] S. R. Nielsen, Q. Zhou, B. Basu, M. T. Sichani, and M. M. Kramer. Optimal control of an array of non-linear wave energy point converters. *Ocean Engineering*, 88:242 – 254, 2014.

[42] I. Noad and R. Porter. Optimisation of arrays of flap-type oscillating wave surge converters. *Applied Ocean Research*, 50:237 – 253, 2015.

[43] M. Penalba, I. Touzn, J. Lopez-Mendia, and V. Nava. A numerical study on the hydrodynamic impact of device slenderness and array size in wave energy farms in realistic wave climates. *Ocean Engineering*, 142:224 – 232, 2017.

[44] E. Renzi, A. Abdolali, G. Bellotti, and F. Dias. Wave-power absorption from a finite array of oscillating wave surge converters. *Renewable Energy*, 63:55 – 68, 2014.

[45] E. Renzi and F. Dias. Relations for a periodic array of flap-type wave energy converters. *Applied Ocean Research*, 39:31 – 39, 2013.

[46] J. V. Ringwood and U. A. Korde. *Hydrodynamic Control of Wave Energy Devices*. Cambridge University Press, 2016.

[47] D. Sarkar, E. Contal, N. Vayatis, and F. Dias. Prediction and optimization of wave energy converter arrays using a machine learning approach. *Renewable Energy*, 97:504 – 517, 2016.

[48] C. Sharp and B. DuPont. Wave energy converter array optimization: A genetic algorithm approach and minimum separation distance study. *Ocean Engineering*, 163:148 – 156, 2018.

[49] J. Singh and A. Babarit. A fast approach coupling boundary element method and plane wave approximation for wave interaction analysis in sparse arrays of wave energy converters. *Ocean Engineering*, 85:12 – 20, 2014.

[50] A. Sinha, D. Karmakar, and C. G. Soares. Performance of optimally tuned arrays of heaving point absorbers. *Renewable Energy*, 92:517 – 531, 2016.

[51] M. C. Sousounis, L. K. Gan, A. E. Kiprakis, and J. K. H. Shek. Direct drive wave energy array with offshore energy storage supplying off-grid residential load. *IET Renewable Power Generation*, 11(9):1081–1088, 2017.

[52] Z. Y. Tay and V. Venugopal. Hydrodynamic interactions of oscillating wave surge converters in an array under random sea state. *Ocean Engineering*, 145:382 – 394, 2017.

[53] G. P. Thomas and D. V. Evans. Arrays of three-dimensional wave-energy absorbers. *Journal of Fluid Mechanics*, 108:6788, 1981.

[54] C. V. Weiss, R. Guanche, B. Ondiviela, O. F. Castellanos, and J. Juanes. Marine renewable energy potential: A global perspective for offshore wind and wave exploitation. *Energy Conversion and Management*, 177:43 – 54, 2018.

[55] H. Wolgamot, P. Taylor, and R. E. Taylor. The interaction factor and directionality in wave energy arrays. *Ocean Engineering*, 47:65 – 73, 2012.

[56] H. Wolgamot, R. E. Taylor, and P. Taylor. Effects of second-order hydrodynamics on the efficiency of a wave energy array. *International Journal of Marine Energy*, 15:85 – 99, 2016. Selected Papers from the European Wave and Tidal Energy Conference 2015, Nante, France.

[57] WorldEnergyCouncil. World energy resources, marine energy 2016. 2016.

[58] S. Zou, O. Abdelkhalik, R. Robinett, G. Bacelli, and D. Wilson. Optimal control of wave energy converters. *Renewable Energy*, 103:217 – 225, 2017.